

Low Driving Voltage of Twisted Nematic Liquid Crystal Displays Doped with CdS Nanoparticles

Yukou Du and Naoki Toshima*

Department of Materials Science and Environmental Engineering, Tokyo University of Science, Yamaguchi, SanyoOnoda 756-0884

Advanced Materials Institute, Tokyo University of Science, Yamaguchi, SanyoOnoda 756-0884

Received April 2, 2007; E-mail: toshima@ed.yama.tus.ac.jp

CdS nanoparticles with size of 2.5 ± 0.4 nm were prepared by using well-known reverse micelle methods. The CdS particles were characterized with ultraviolet and visible (UV–vis) absorption spectroscopy, transmission electron microscopy (TEM), energy-disperse X-ray analysis (EDX), Fourier transform infrared (FT-IR), and X-ray diffraction (XRD). Twisted nematic liquid crystal display (TN-LCD) devices, doped with various amount of CdS nanoparticles, were studied for the first time. The results showed that electro-optic characteristics were featured by a frequency modulation. As the amount of dopant increased, a wider frequency response was achieved. Interestingly, the driving voltage of TN-LCD decreased as 4′-pentylbiphenyl-4-carbonitrile (4′-pentyl-4-cyanobiphenyl, 5CB) was doped with CdS nanoparticles.

In recent years, liquid crystal displays (LCDs) have been applied to informational and visual equipments, including personal computers, as thin, light, and low power-consuming flat panel displays. LCDs are indispensable devices for the progress of visual-information society. Electro-optic effects in a twisted nematic liquid crystal display (TN-LCD) cell are important and of interest in the fields of both basic materials science and device applications.[1,2] On the other hand, science and technology involving nanomaterials have received much attention recently.[3–12]

With regards to liquid crystals, many reports have been published on nano-structured liquid crystals, containing, for example, nanostructure formation by gelation of liquid crystals,[13,14] nano-droplets in nematic phase,[15] and stabilization of chiral smectic phase.[16] Introducing nanomaterials and nanotechnology into electro-optic (EO) device technology, such as LCDs, can provide the frequency modulation and improve the response time peculiarly. In our previous studies, TN-LCDs of 4′-pentylbiphenyl-4-carbonitrile (so called "5CB," K-15 by Merck. Hereafter, 5CB will be used in this paper based on conventional nomenclature, 4′-pentyl-4-cyanobiphenyl.), fabricated by doping with metal nanoparticles, such as Pd,[17,18] Ag,[19] and Ag–Pd,[20] have been shown to exhibit a frequency modulation electro-optic response with a short response time. The frequency range spreads from 40 Hz to 2 kHz around a dielectric relaxation frequency that increases with increasing the concentration of metal nanoparticles.

As another kind of nanomaterials, semiconductor nanoparticles play a major role in several new technologies. Intense interest in this area is derived from their unique chemical, physical, and electronic properties,[21–24] which make them useable in the fields of displays, lighting, sensors, and lasers, as well as other areas. CdS nanoparticles,[25–27] which are important 12–16 group semiconductors, has been extensively studied due to its potential applications, in such things as field effect transistors, light-emitting diodes, photocatalysis, and biological sensors. In this paper, nearly monodispersed CdS nanoparticles were synthesized in reverse micelle solution. TN-LCD devices doped with CdS nanoparticles were studied. Doped with 0.2 wt % CdS nanoparticles, the lowest driving voltage of TN-LCD devices was 1.2 V, which is only 66.67% of the value (1.8 V) of TN-LCD devices composed of pure 5CB. To the best of our knowledge, this is the first report about the fabrication of a twisted nematic liquid crystal display doped with semiconductor nanoparticles.

Experimental

Synthesis of CdS Nanoparticles. The CdS nanoparticles were prepared by mixing two reverse micelle systems.[28,29] The first reverse micelle system was prepared by mixing 50 mL of heptane, 0.5 g of sodium bis(2-ethylhexyl)sulfosuccinate (Aerosol OT®, AOT) and 0.035 mL of 0.05 mol L^{-1} $CdCl_2$ aqueous solution in a vessel with a magnetic stirrer until a colorless transparent solution was obtained. The second one was prepared by mixing 50 mL of heptane, 0.5 g of AOT, and 0.035 mL of 0.05 mol L^{-1} Na_2S aqueous solution. A transparent solution was obtained after adding the second system to the first one in a reaction flask and stirring for 30 min. Then, 40 mL of the above transparent solution was mixed with 40 mg of 1-hexadecanethiol (HDT) under stirring for 3 h. The obtained micelle solution was added to 150 mL of pure water in a separatory funnel and kept in the funnel in a stable state. AOT was gradually dissolved in the water layer, which became nontransparent and was replaced by fresh pure water. The washing was repeated until the water layer was transparent. In the washing process, the amount of AOT decreased gradually, and finally HDT replaced AOT completely as the protector. Colloidal dispersions of the HDT-protected CdS nanoparticles were very stable and colorless.

Fabrication of TN-LCD Cell. 5CB (0.05 g) in 20 mL of heptane was mixed with 2 mL of colloidal dispersions of the CdS nanoparticles in heptane by stirring for 1 h. The heptane in

Published on the web December 13, 2007; doi:10.1246/bcsj.80.2446

the mixture was then slowly evaporated by a rotary evaporator. Finally, the residual heptane and free HDT were removed by a vacuum evaporation method, and 5CB doped with CdS nanoparticles was obtained. TN-LCDs were fabricated by injecting the 5CB doped with CdS nanoparticles into a TN cell with a cell gap of 5.1 μm.

Measurements. UV–vis spectra were recorded at room temperature using a Shimadzu 2500PC spectrophotometer equipped with a 10 mm quartz cell in the wavelength range of 300–550 nm. Transmission electron microscopy (TEM) and energy-disperse X-ray analysis (EDX) measurements were performed on a TECNAI-12 instrument (Philips) operated with an accelerating voltage of 120 kV. X-ray diffraction (XRD) was performed on a Rigaku Rint 2000 X-ray diffractometer with Cu Kα radiation at 40 kV and 100 mA. Infrared spectra were recorded on a JIR-WINSPEC 50 Fourier transform infrared (FT-IR) spectrophotometer. The electro-optic characteristics (V–T curves) of the sample cells were measured using a measuring instrument (Ohtsuka, Model LC-5200) and an in-house instrument using the frequencies as a parameter. Finally, the initial driving voltages and response times of TN-LCDs were determined for various doping amounts of the CdS nanoparticles.

Results and Discussion

Preparation and Characterization of HDT-Caped CdS Nanoparticles. The CdS nanoparticles were prepared by mixing AOT protected $CdCl_2$ and Na_2S, then HDT was added in the reverse micelle system. AOT was replaced gradually by HDT in the succeeding wash process. In our experiment, HDT was firstly used to synthesize directly CdS nanoparticles, and the obtained nanoparticles had a large size distribution.

TEM image and size distribution of the HDT-caped CdS nanoparticles prepared through the replacement processes are shown in Fig. 1. The CdS nanoparticles were spherical and nearly monodispersed based on the TEM observation. The average particle size and the standard deviation were 2.5 and 0.4 nm, respectively.

Energy-disperse X-ray analysis (Fig. 2) indicates the presence of C, S, and Cd, supporting the presence of CdS. The average molar ratio of S to Cd was 2.1, giving the higher intensity of "S" than "Cd." It should be related to sulfur from the protected thiols.

Figure 3 shows the UV–vis spectrum of the HDT-caped CdS nanoparticles. The maximum absorption of CdS nanoparticles appears at 385 nm, which is significantly blue-shifted

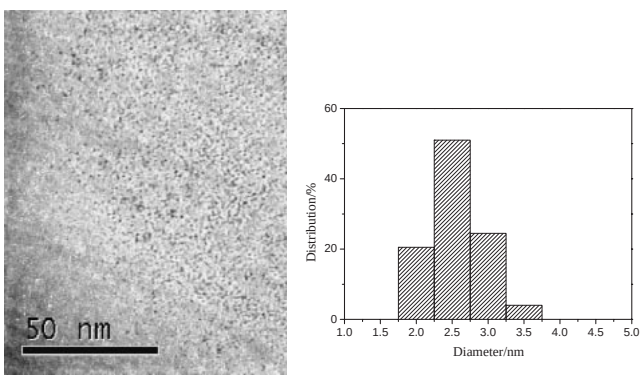

Fig. 1. TEM photograph and size distribution of the thiol-caped CdS nanoparticles.

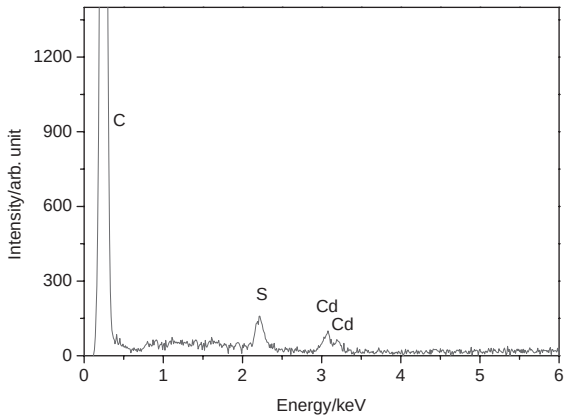

Fig. 2. Energy-disperse X-ray analysis of the thiol-caped CdS nanoparticles.

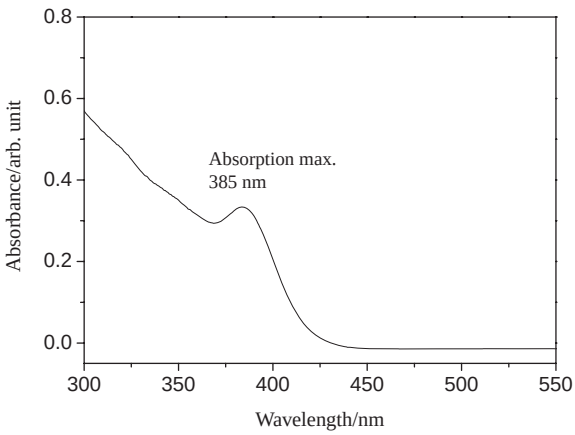

Fig. 3. UV–vis spectrum of the HDT-caped CdS nanoparticles.

compared with that of bulk CdS (515 nm). It is considered to be due to quantum confinement effects.[30] It is well known that the diameter of the particles is correlated with the absorption wavelength at the edge[31,32] and the size of the nanoparticles can be calculated by using the Eq. 1:

$$2R_{CdS} = 0.1/(0.1338 - 0.0002345\lambda_e) \text{ (nm)}, \quad (1)$$

where R_{CdS} and λ_e are the diameter of particles and absorption wavelength at the edge, respectively. λ_e is calculated from the intersection of the sharply decreasing line of the spectrum with the baseline.[31] Since λ_e was 410 nm in the UV–vis spectrum, the diameter of the CdS nanoparticles was calculated to be 2.6 nm. This value is in good agreement with that observed on the TEM image.

FT-IR spectra of HDT and HDT-protected CdS are shown in Fig. 4. The spectrum of HDT-protected CdS is very similar to that of pure HDT. A typical stretching band due to the CO group of AOT (at 1736 cm^{-1}) completely disappeared, which means that AOT is completely replaced by HDT.

XRD patterns of pure 5CB and CdS-doped 5CB are shown in Fig. 5. For the 0.1 wt % CdS-doped sample, the peaks attributed to CdS could not be detected, because the content of CdS was very low. For the 1 wt % CdS-doped sample, characteristic peaks for CdS appeared at 26.6°, although the intensity was very weak.

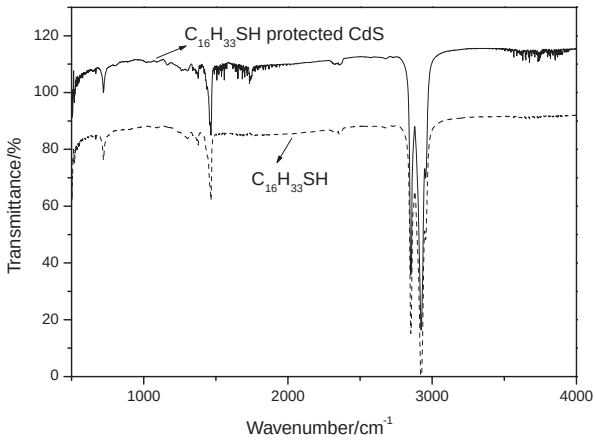

Fig. 4. FT-IR spectra of HDT and HDT-protected CdS.

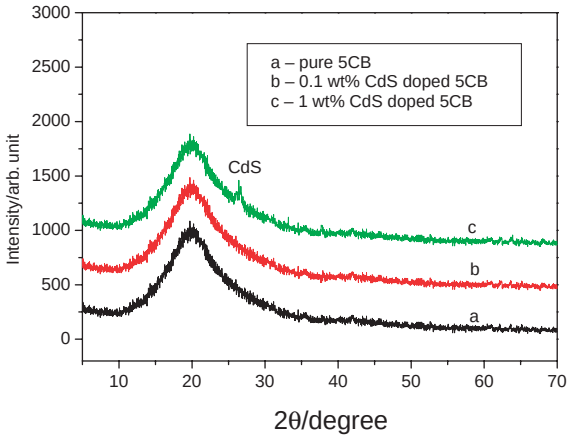

Fig. 5. XRD patterns of pure 5CB and CdS-doped 5CB.

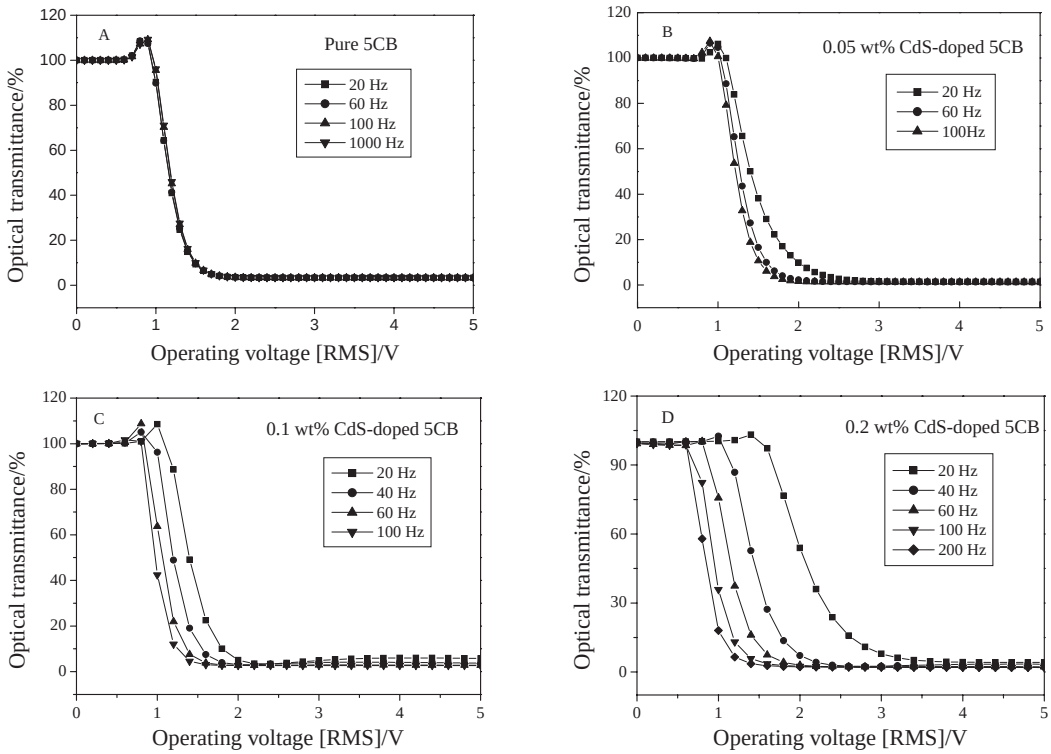

Fig. 6. Frequency modulation patterns of the TN-LCD devices using pure 5CB and CdS-doped 5CB.

Frequency Modulation of TN-LCD Devices Using CdS-Doped 5CB. The *T*–*V* curves of TN-LCD devices using pure 5CB and CdS-doped 5CB are shown in Fig. 6. The TN-LCDs using CdS-doped 5CB clearly showed frequency modulation, whereas that using pure 5CB did not even in the wide frequency range from 20 to 1000 Hz (Fig. 6A). For the 0.05 wt % CdS-doped sample, the frequency modulation range was from 20 to 100 Hz (Fig. 6B). As the doping amount of CdS nanoparticles was increased, the frequency modulation range increased. For the 0.1 wt % CdS-doped sample, the increment was not so evident, being still in the range from 20 to 100 Hz (Fig. 6C). For the 0.2 wt % CdS-doped sample, however, the largest range from 20 to 200 Hz was achieved in the present study (Fig. 6D). When the doping ratio of CdS was increased to 0.3 wt %, the appearance of the doped cell changed obviously by heat treatment at 80 °C for 24 h, indicating the 0.3 wt % CdS-doped sample does not have a sufficient lifetime.

Metallic nanoparticle-doped samples also showed a similar frequency modulation, as previously reported by us.[17–20] The frequency modulation effect is mainly explained by the conductivity of metallic nanoparticles.[20] The conductivity of CdS nanoparticles may be much lower than that of metal nanoparticles. In the present work, the frequency modulation range is more narrow than that of metal nanoparticle-doped sample. Therefore, the narrower range is probably due to the poor conductivity of the CdS nanoparticles.

Driving Voltage of TN-LCD Devices Using CdS-Doped 5CB. Figure 7 shows the time-dependent transmission changes of TN-LCD devices using pure 5CB and CdS-doped 5CB, as a function of an applied voltage. Nematic liquid crys-

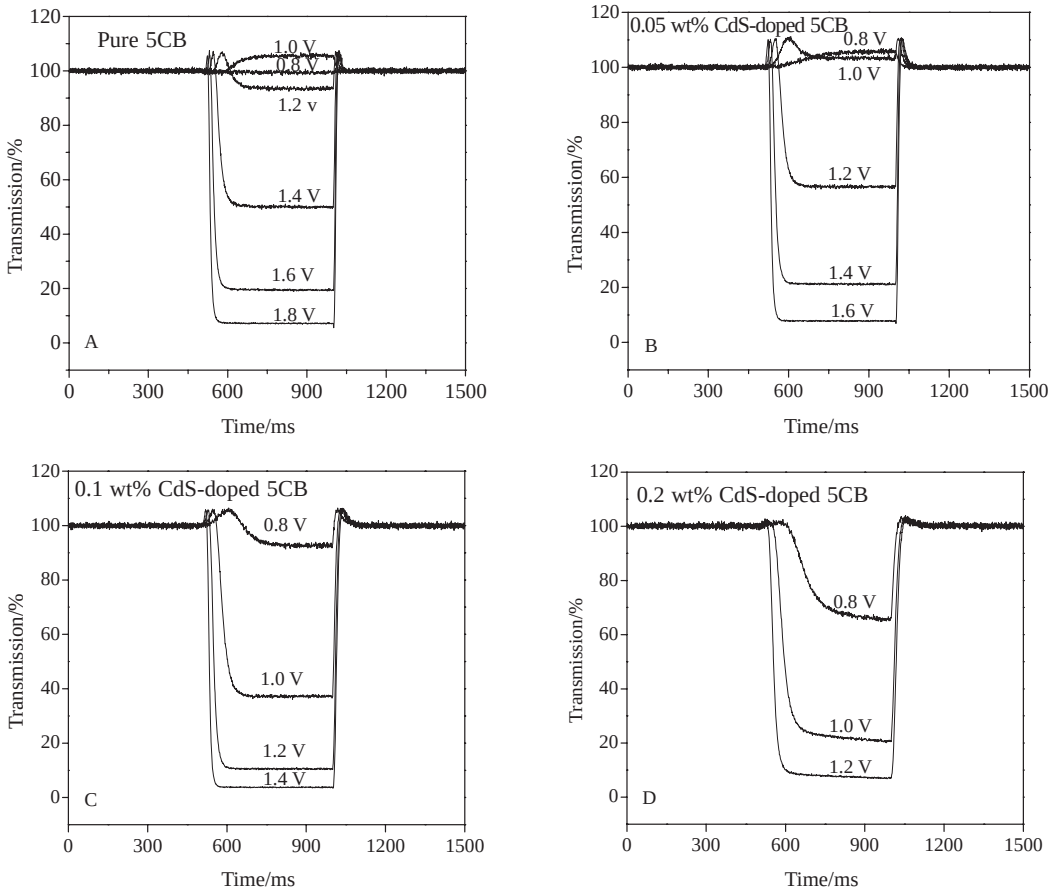

Fig. 7. The lowest driving voltages of the TN-LCD devices using pure 5CB and CdS-doped 5CB.

talline 5CB in the TN-LCD device orientates under the influence of external electric field. Therefore, the TN-LCD device switches from a transparent state to an opaque one for a polarized light when external voltage is applied, resulting in a gradual decrease in transmission. Usually, a external voltage at 10% transmission is defined as the lowest driving voltage. As shown in Fig. 7, the lowest driving voltage of the TN-LCD devices using the pure 5CB was 1.8 V. On the other hand, the lowest driving voltages of 0.05, 0.1, and 0.2 wt % CdS-doped 5CB were 1.6, 1.4, and 1.2 V, respectively. Interestingly, the lowest driving voltage of TN-LCD devices using CdS-doped 5CB was lower than that of pure 5CB. The lowest driving voltage decreased with an increase in the amount of doped CdS nanoparticles.

It is noteworthy that TN-LCDs fabricated with metal nanoparticle-doped 5CB showed an increase in the lowest driving voltages with an increase in the doping amount of the metallic nanoparticles.[17–20] The increase in the lowest driving voltage in the case of metal nanoparticle-doped 5CB has been explained by the increase in the apparent dielectric anisotropy using Maxwell–Wagner theory. In the case of MgO and SiO_2 nanoparticle-doped TN-LCD, in contrast, the Maxell–Wagner theory cannot be applied, and the decrease in the lowest driving voltage can be explained by the decrease in the order parameter.[33] Thus, in the case of CdS nanoparticles, an explanation similar to the case of MgO and SiO_2 could be useful. Anyway, it is emphasized that the decrease in the lowest driving voltage of the TN-LCDs using the CdS-doped 5CB is advantageous for reducing and saving energy.

As for the response time, the present system is very complicated. The response time for rising decreased by doping 5CB with 0.05 wt % CdS nanoparticles, as shown in Fig. 8A. There was a greater decrease when the amount of dopant was increased from 0.05 to 0.1 wt %; however, the value reached a minimum at this point, resulting in a constant. In contrast, the response time for falling could not be improved at all. Thus, the total response time (Fig. 8B) was effected by two opposite factors. For the sample with a low doping level, a little faster response was observed due to quick rising response. For the samples with a high doping level, in contrast, the total response became worse due to slow falling response. Further study is in progress to understand these complicated phenomena.

Conclusion

In summary, nearly monodispersed HDT-protected CdS nanoparticles were prepared by using well-known reverse micelle methods, followed by replacement of the micelle. The TN-LCD devices fabricated by CdS-doped 5CB showed a decrease in the lowest driving voltage with an increase in the doping amount of the CdS nanoparticles, coupled with frequency modulation. The decrease in the driving voltage can be extended to the development of new display devices with low energy requirement.

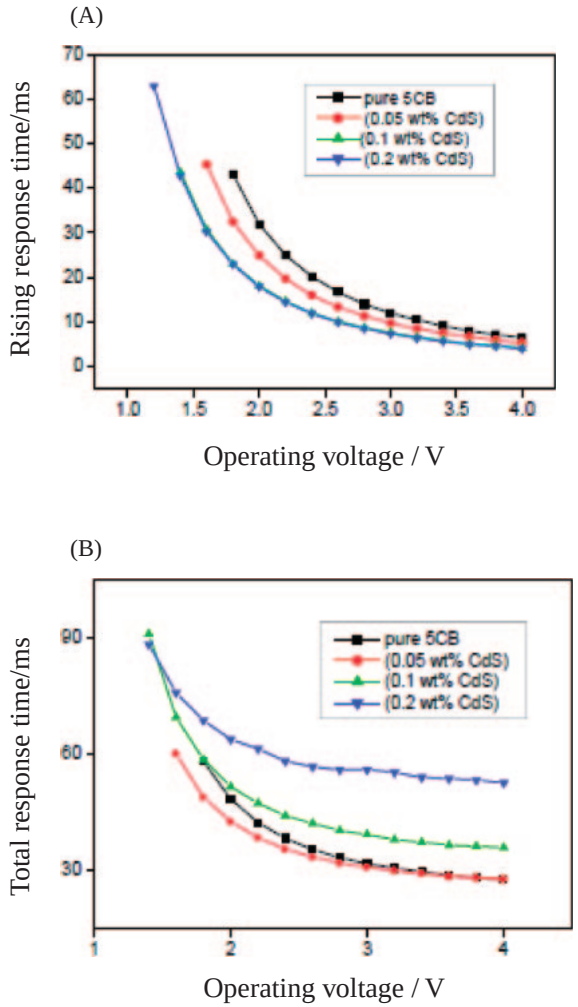

Fig. 8. (A) The rising response time of none, 0.05, 0.1, and 0.2 wt % CdS nanoparticle-doped 5CB cells at various operating voltages. (B) The total response time of none, 0.05, 0.1, and 0.2 wt % CdS nanoparticle-doped 5CB cells at various operating voltages.

This work is supported by a Consortium R&D Project for Regional Revitalization from METI, Japan, and a Cooperation Project for Innovative Technology and Advanced Research in Evolutional Area (City Area) from MEXT, Japan. The authors are grateful to Prof. S. Kobayashi, Dr. H. Yan, and Mr. N. Nishida at TUSY for their kind discussion and help in this work.

References

1 S. Kobayashi, H. Hori, Y. Tanaka, in *Handbook of Liquid Crystal Research*, ed. by P. J. Collings, J. S. Patel, Oxford University Press, New York, **1997**, Chap. 10.

2 L. M. Blinov, V. G. Chigrinov, *Electrooptic Effects in Liquid Crystal Materials*, Springer, New York, **1994**.

3 *Nanoparticles: From Theory to Application*, ed. by G. Schmid, Wiley-VCH, Weinheim, **2004**.

4 *Macromolecular Nanostructured Materials*, ed. by N. Ueyama, A. Harada, Kodansha/Springer, Tokyo/Berlin, **2004**.

5 P. Lu, J. Dong, N. Toshima, *Langmuir* **1999**, *15*, 7980.

6 S. Link, Z. L. Wang, M. A. El-Sayed, *J. Phys. Chem. B* **1999**, *103*, 3529.

7 S. Sun, C. B. Murray, D. Weller, L. Folks, A. Moser, *Science* **2000**, *287*, 1989.

8 T. Teranishi, M. Miyake, *Chem. Mater.* **1999**, *11*, 3414.

9 N. Toshima, T. Yonezawa, *New J. Chem.* **1998**, *22*, 1179.

10 N. Toshima, T. Takahashi, H. Hirai, *Chem. Lett.* **1987**, 1031.

11 N. Toshima, Y. Shiraishi, T. Teranishi, M. Miyake, T. Tominaga, H. Watanabe, W. Brijoux, H. Bönnemann, G. Schmid, *Appl. Organomet. Chem.* **2001**, *15*, 178.

12 N. Toshima, Y. Shiraishi, T. Teranishi, *J. Mol. Catal. A: Chem.* **2001**, *177*, 139.

13 N. Mizoshita, K. Hanabusa, T. Kato, *Adv. Mater.* **1999**, *11*, 392.

14 N. Mizoshita, K. Hanabusa, T. Kato, *Adv. Funct. Mater.* **2003**, *13*, 313.

15 J. Fukuda, H. Yokoyama, *Eur. Phys. J. E* **2006**, *21*, 341.

16 H. Fujikake, H. Sato, T. Murashige, *Displays* **2004**, *25*, 3.

17 H. Yoshikawa, K. Maeda, Y. Shiraishi, J. Xu, H. Shiraki, N. Toshima, S. Kobayashi, *Jpn. J. Appl. Phys.* **2002**, *41*, L1315.

18 Y. Shiraishi, N. Toshima, K. Maeda, H. Yoshikawa, J. Xu, S. Kobayashi, *Appl. Phys. Lett.* **2002**, *81*, 2845.

19 J. Thisayukta, H. Shiraki, Y. Sakai, T. Masumi, S. Kundu, Y. Shiraishi, N. Toshima, S. Kobayashi, *Jpn. J. Appl. Phys.* **2004**, *43*, 5430.

20 Y. Sakai, N. Nishida, H. Shiraki, Y. Shiraishi, T. Miyama, N. Toshima, S. Kobayashi, *Mol. Cryst. Liq. Cryst.* **2005**, *441*, 143.

21 A. P. Alivisatos, *Science* **1996**, *271*, 933.

22 S. M. Lee, Y. W. Jun, S. N. Cho, J. Cheon, *J. Am. Chem. Soc.* **2002**, *124*, 11244.

23 Y. W. Jun, Y. Y. Jung, J. Cheon, *J. Am. Chem. Soc.* **2002**, *124*, 615.

24 J. He, I. Ichinose, T. Kunitake, A. Nakao, Y. Shiraishi, N. Toshima, *J. Am. Chem. Soc.* **2003**, *125*, 11034.

25 P. S. Chowdhury, P. Sen, A. Patra, *Chem. Phys. Lett.* **2005**, *413*, 311.

26 U. K. Gautam, M. Ghosh, C. N. R. Rao, *Chem. Phys. Lett.* **2003**, *381*, 1.

27 U. K. Gautam, R. Seshadri, C. N. R. Rao, *Chem. Phys. Lett.* **2003**, *375*, 560.

28 P. Lianos, J. K. Thomas, *Chem. Phys. Lett.* **1986**, *125*, 299.

29 P. Lianos, J. K. Thomas, *J. Colloid Interface Sci.* **1987**, *117*, 505.

30 L. Spanhel, H. Haase, H. Weller, A. Henglein, *J. Am. Chem. Soc.* **1987**, *109*, 5649.

31 M. Moffitt, A. Eisenberg, *Chem. Mater.* **1995**, *7*, 1178.

32 R. He, X. Qian, J. Yin, H. Xi, L. Bian, Z. Zhu, *Colloids Surf., A* **2003**, *220*, 151.

33 F. Haraguchi, K. Inoue, N. Toshima, S. Kobayashi, K. Takatoh, *Jpn. J. Appl. Phys.* **2007**, *46*, L796.